EMC3-EIRENE modelling of toroidally-localized divertor gas injection experiments on Alcator C-Mod

J.D. Lore*[a], M.L. Reinke[b], B. LaBombard[c], B. Lipschultz[b], R.M. Churchill[c], R.A. Pitts[d], Y. Feng[e]

[a]*Oak Ridge National Laboratory, Oak Ridge, TN 37831, USA*
[b]*York Plasma Institute, Department of Physics, University of York, Heslington, York YO10 5DD, UK*
[c]*Plasma Science and Fusion Center, MIT, Cambridge, MA 02139, USA*
[d]*ITER Organization, Route de Vinon sur Verdon, 13115 Saint Paul Lez Durance, France*
[e]*Max Planck Institute for Plasma Physics, Greifswald, Germany.*

Abstract

Experiments on Alcator C-Mod with toroidally and poloidally localized divertor nitrogen injection have been modeled using the three-dimensional edge transport code EMC3-EIRENE to elucidate the mechanisms driving measured toroidal asymmetries. In these experiments five toroidally distributed gas injectors in the private flux region were sequentially activated in separate discharges resulting in clear evidence of toroidal asymmetries in radiated power and nitrogen line emission as well as a ~50% toroidal modulation in electron pressure at the divertor target. The pressure modulation is qualitatively reproduced by the modelling, with the simulation yielding a toroidal asymmetry in the heat flow to the outer strike point. Toroidal variation in impurity line emission is qualitatively matched in the scrape-off layer above the strike point, however kinetic corrections and cross-field drifts are likely required to quantitatively reproduce impurity behavior in the private flux region and electron temperatures and densities directly in front of the target.

PACS: 52.25.Vy 52.25.Ya 52.65.Pp 52.55.Rk

PSI-21 Keywords: Alcator C-Mod, Divertor Detachment, Divertor Modelling, Edge Monte Carlo

Corresponding Author Address:

Oak Ridge National Laboratory

1 Bethel Valley Rd

Oak Ridge TN, 37831

Corresponding Author e-mail: lorejd@ornl.gov

Presenting Author: J.D. Lore

Presenting Author e-mail: lorejd@ornl.gov

1. Introduction

Future fusion reactors such as ITER are envisioned to operate with partially detached divertor conditions to reduce the peak power flux density carried to the plasma-facing components (PFCs) while maintaining H-mode core confinement [1]. During burning plasma operation, ITER will rely on extrinsic impurity (such as N_2, Ne, Ar) seeding provided by a set of gas valves below the divertor cassettes spaced equally toroidally around the torus [2]. To investigate the potential for asymmetry introduced by a small number of toroidally localized gas injection locations, experiments were performed on the Alcator C-Mod tokamak [3] in which five toroidally distributed gas injectors located in the private flux region (PFR) were sequentially activated in separate (otherwise similar) discharges. Clear evidence of toroidal asymmetries, e.g., in nitrogen line emission, radiated power, and divertor electron pressure, was found by comparing toroidally fixed diagnostic data relative to the toroidal position of the puff. As a result of these experiments the ITER system was expanded to six gas injection locations from the originally foreseen three.

Even with six injectors toroidal asymmetries may exist in ITER, motivating predictive modeling validated on the C-Mod results. This paper documents an attempt to benchmark three dimensional simulations of the C-Mod experiments using the 3D plasma boundary transport code EMC3-EIRENE [4,5], which is a coupling of Monte Carlo fluid transport (EMC3) with kinetic neutral particle recycling and transport (EIRENE).

2. Experimental conditions

The experiment was performed over a set of deuterium main ion lower single null Ohmic L-mode plasmas (C-Mod shots 109814005-109814016) where the ∇B drift direction was towards the X-point. A brief overview of the experiment is given here, with a more complete description to be reported elsewhere [6]. A control shot without N_2 puff was first run (plasma current I_p=1 MA, toroidal field strength B_t=5.5T, safety factor q_{95}=3.75, core electron density $n_e \sim 2.3 \cdot 10^{20}$ m^{-3}, Ohmic power P_{oh}=1.5MW, power radiated inside the separatrix $P_{rad\text{-}core}$=0.25MW) with outer divertor conditions observed to be in the high recycling regime. In subsequent discharges nitrogen is injected in the PFR (see Fig. 1 inset) from a set of toroidally spaced gas capillary tubes at $t \approx 0.8$s, and enters the vacuum

chamber over approximately 0.5s. Each gas position was used in two separate shots, demonstrating reproducible toroidal trends. An example is given in Figure 2a, which shows the change in the line-averaged brightness of the 494.5 nm N V emission at the X-point with respect to the pre-puff value, normalized to the total gas injected. The colors indicate the diagnostic position relative to the toroidal angle of the active puff, with the dashed and solid lines of the same color indicating the two shots with the same gas location. Note that the signals never reach a steady-state, to compare to the simulation results an average is taken around the peak value (shaded region). Figure 2b shows the change in N V line brightness averaged over the peak for the ten shots relative to the puff.

3. Setup of EMC3-EIRENE simulations

EMC3 solves the three-dimensional steady-state plasma continuity, parallel momentum, and electron and ion energy fluid equations using a Monte Carlo method [3]. The fluid transport is classical [7] parallel to field lines while the cross-field transport is taken to be diffusive with user-specified particle and heat diffusivities. Cross-field drifts and kinetic corrections in the form of flux limiters [8] are not included. The particle, momentum and energy source terms due to plasma-neutral interactions are calculated by EIRENE. Volume recombination is neglected in the version of the code used here; however it has recently been included in some EMC3-EIRENE simulations [9].

The experiments were modeled using shot 1090814013 with the background magnetic equilibrium taken from EFIT [10] calculations at t=743ms. The simulation domain spans the entire torus in five toroidal domains with a toroidal grid resolution of 2°. A 2D cut of the grid is shown in Fig. 1, with the inset showing the increased resolution near the target plates and the separatrix ($\Delta_{R,Z}$ ~ 1mm). In the toroidal direction the cells are aligned with the magnetic field. The grid is divided into three computational 'blocks' [11], core (black), scrape-off layer (SOL) (red) and PFR (blue), with thick black lines indicating toroidally symmetric molybdenum PFCs included in the simulation with a main ion recycling coefficient of unity. Green cells indicate 'target' cells at which sheath boundary conditions are applied ($V_\parallel = c_s \equiv \sqrt{(T_e + T_i)/m_i}$, $q_a = \gamma_a T_a c_s, \gamma_e = 4.5, \gamma_i = 2.5$, where $V_\parallel$ is the parallel plasma velocity, c_s is the ion sound speed, and q_a and γ_a are the heat flux and sheath heat

transmission coefficient of species *a*). Core boundary conditions are taken from experiment, n_{core} = $1.1 \cdot 10^{20}$ m^{-3}, $P_{core} = P_{OH} - P_{rad}^{core}$ = 1.25MW, and decay length boundary conditions of λ_e, λ_p=3cm, λ_m=200m for energy, particles and momentum, respectively are used at the outer radial boundaries (the grid is extended radially until the simulation is insensitive to the decay lengths). A cross-field thermal diffusivity of $\chi_\perp$ = 1 m^2/s and main and impurity ion particle diffusivity of $D_\perp$ =0.3 m^2/s are used.

The gas puff is included in the simulation by sourcing atomic nitrogen at R=60.5 cm, Z=-59 cm, (see Fig 1 inset), with an initial energy of 1eV and an isotropic velocity distribution. The source intensity is taken from puff calibration shots ($N_0=2N_2$) $S_N = e\Gamma_N$ =105A, and the impurity recycling coefficient is R=0.5. Impurity transport is performed for a trace fluid species ($Z_a n_a << n_i$) with $T_a=T_i$ using a recent version of EMC3 which allows for recycling impurities [12]. The impurity ion force balance includes contributions from the impurity pressure gradient, main ion friction, electrostatic force, electron temperature gradient, and ion temperature gradient [13]. The impurity species feeds back into the main plasma solution through a cooling term in the electron energy equation, which accounts for ionization and excitation radiation.

4. Comparison to experimental profiles

The upstream (separatrix) values of the electron density and temperature from the simulation are approximately matched to the experimental data by specifying spatially constant cross-field diffusivities. Figure 3 shows the electron temperature, density and pressure profiles at the outboard midplane ($\rho \equiv R - R_{sep}$) from Thomson scattering (symbols with error bars) and EMC3-EIRENE (solid lines).

The electron kinetic profiles at the outer target are shown mapped to the outboard midplane in Figure 4. The Langmuir probe (circles) and EMC3-EIRENE (solid lines) data are averaged toroidally over the 10 shot series. Langmuir probe densities and heat fluxes near the strike point have been suppressed due to possible contamination from the 'death-ray' effect [14]. Red crosses in the Fig. 4c are upstream data from Thomson scattering. The target electron pressure in the SOL agrees within factor of ~2; however the simulations underestimate T_e and overestimate n_e near the strike point. It is

possible the pressure match could be improved by better matching the upstream pressure, however 2D fluid simulations have also consistently predicted colder, denser target conditions as compared to experiment [15], which has been attributed to the neglect of kinetic effects, e.g., parallel heat flux carried by supra-thermal electrons. The overall discrepancy might be expected to be larger in EMC3 which also neglects parallel momentum and heat flux kinetic corrections in the form of flux limiters, which are included in the 2D simulations. An attempt has been made previously to iteratively include flux limiters in EMC3 [16], however the results were not able to be consistently applied in a stable fashion. Future extensions to the code may include inclusion of flux limiters directly into the Monte Carlo process [16]. Here we will focus on qualitative comparisons with a goal of understanding the mechanisms driving the toroidal asymmetries in the C-Mod experiment. Future simulations will attempt to match the downstream conditions by reducing the density at the separatrix.

In both simulations and experiment the inclusion of the localized nitrogen gas puff results in a toroidal modulation of the electron pressure at the divertor near the strike point. The fractional change in the pressure as compared to the pre-puff pressure at $\rho \approx 3$mm is shown in Fig. 5 as a function of the relative puff position. Both the experimental and the simulated toroidal modulation has a qualitative $n \approx 1$ structure. In the simulation this modulation is due to a torodial varation in the plasma-neutral momentum sinks (ionization and charge-exchange), caused by local reduction in the electron temperature (and therefore the rate coefficients) due to the asymmetric nitrogen power radiation in flux tubes connecting to the target near the strike point, as discussed in the next section.

5. Impurity dynamics and comparison to spectroscopic data

The wide range of vacuum ultraviolet and visible spectroscopy diagnostics available on Alcator C-Mod show the 3D structure of the nitrogen line emission. Here we will focus on N V line emission to characterize the impurity dynamics with more experimental results shown in [6]. The plasma in the divertor 'slot', 57 cm < R < 62 cm and Z < -51 cm, has a very low electron temperature (~1eV) resulting in nitrogen ionization mean free paths on the scale of meters. A significant portion of the neutral nitrogen is ionized along and above the outer separatrix leg where T_e is larger, with ionization front of each higher charge state nearer to the x-point and higher above the separatrix leg.

The N^{+4} density at the toroidal angle of the puff is shown in Fig. 6 along with the lines of sight for three fibers that view above, through and below the x-point.

Figure 7 shows the toroidal variation in N V line emission relative to the puff position from for the three views. The simulated data is calculated by integrating the N^{+4} density along the diagnostic lines of sight, a procedure which is expected to give meaningful qualitative comparisons. The trends in the modeled data can be understood by examining the parallel forces acting on the impurity ions. The dominant forces in this region are the main ion friction (dominantly acting towards the targets) and the main ion temperature gradient (acting away from the targets). In the SOL above the outer strike point, the gradient force is larger, and the impurities are 'pushed' upstream into the view for toroidal angles away from the puff, resulting in a minimum near $\phi = 0$ (Fig. 7a). For the x-point view the main ion friction dominates in the SOL, pulling the impurity ions out of the view resulting in a maximum near $\phi = 0$ (Fig. 7b). The asymmetry about $\phi = 0$ occurs because the flux tubes in the positive ϕ direction (clockwise when viewing the machine from above) are intercepted by the target. Finally, for the view below the x-point the main ion friction pulls the ions into the view towards the positive ϕ. The peak occurs at positive ϕ due to the larger density along the outer separatrix leg as compared to the inner (Fig. 7c). The experimental data shows similar trends for the first two cases, however the peaking for the view through the x-point is a factor of two smaller than in the simulation, which could be attributed to the lack of a quantitative agreement in the downstream plasma parameters. The below x-point view experimentally peaks near $\phi = 0$, unlike in the simulation. This discrepancy could be due to several sources. The neglect of cross-field drifts is likely to be critical in the PFR, as shown in previous C-Mod results [17,18]. The experiment also had the outer strike point location moving ~4cm along the outer target from 743ms to 1093ms, complicating comparison of views near the strike point location. Future comparisons will focus on experiments with strike point position control to mitigate this issue.

6. Prediction of divertor heat flux asymmetry

The simulations predict a toroidal asymmetry in the heat flux to the outer target, as shown in Fig. 8. The heat flux at the strike point is reduced from the axisymmetric level at toroidal angles where

the flux tubes intersecting the target have localized momentum and power sinks upstream. The toroidal variation in the target heat flux is ~2x, however this effect may be larger in cases where the peak heat flux is not shifted away from the strike point. This prediction has not been confirmed by experimental measurement as the heat flux data from the Langmuir probes is complicated near the strike point due to the 'death ray' effect. New experiments with IR camera views of the outer strike point have been proposed to investigate toroidal asymmetries in the heat flux due to localized gas injection.

7. Summary

Experiments on Alcator C-Mod with toroidally and poloidally localized divertor gas injection have been simulated with EMC3-EIRENE. The up- and downstream electron pressure profiles were approximately matched by specifying cross-field diffusivities, however the simulated divertor plasma is consistently colder and denser than measured. Future extensions to the code to include kinetic corrections may improve the agreement. Alternatively the upstream density could be decreased to better match the downstream conditions. Measured toroidal pressure modulation is qualitatively reproduced by the code, as well as toroidal asymmetry in N V line emission for views through the SOL. Trends in spectroscopic measurements through the PFR are not captured by the simulation. Experiments have been proposed on C-Mod for the next run campaign to perform similar experiments in H-mode plasmas in order to perform further benchmarking and validation of EMC3-EIRENE.

Acknowledgements

The submitted manuscript has been authored by a contractor of the U.S. Government under contracts DE-AC05-00OR22725 and DE-FC02-99ER54512. Accordingly, the U.S. Government retains a nonexclusive, royalty-free license to publish or reproduce the published form of this contribution, or allow others to do so, for U.S. Government purposes. The views and opinions expressed herein do not necessarily reflect those of the ITER Organization.

References

[1] R.A. Pitts, et al., J. Nucl. Mater. 438 (2013) S48.

[2] S. Maruyama, et al., IAEA FEC, San Diego 2012, paper ITR/P5-24.

[3] E.S. Marmar and the Acator C-Mod Group, Fusion Sci. Technol. 51 (2007) 261.

[4] Y. Feng, et al., J. Nucl. Mater., 241 (1997) 930.

[5] Y. Feng, et al., J. Nucl. Mater. 266 (1999) 812.

[6] M.L. Reinke, et al., PSFC Research Report PSFC/RR-14-3, MIT, Cambridge (2014).

[7] S.I. Braginskii, Rev. Plasma Phys., Vol 1 (1965) 205.

[8] P.C. Stangeby, "The Plasma Boundary of Magnetic Fusion Devices", Chapter 26, IOP Publishing, Bristol UK (2000).

[9] H. Frerichs, Personal Communication (2014).

[10] L. Lao, et al., Nucl. Fusion 25 (1985) 1611.

[11] H. Frerichs, et al., Comp. Phys. Comm. 181 (2010) 61.

[12] Y. Feng, et al., 14th PET Conference (2014), submitted to Contrib. Plasma Phys.

[13] Y. Feng, et al., Comp. Phys. Comm 184 (2013) 1555.

[14] D. Brunner, et al., J. Nucl. Mater 483 (2013) S1196

[15] A. Chankin, et al., Nucl. Fusion 49 (2009) 015004

[16] D. Harting, et al., Contrib. Plasma Phys. 48 (2008) 99

[17] Smick et al., Nucl. Fusion 53 (2013) 023001

[18] Boswell et al., J. Nucl. Mater. 290 (2001) 556.

Figure Captions

Figure 1: 2D cut of the EMC3-EIRENE grid.

Figure 2: a) Change in N V line brightness after gas injection for five toroidal positions relative to the puff location, b) average change in brightness from the shaded time region versus toroidal position relative to puff.

Figure 3: Radial profiles at the outboard midplane of a) T_e, b) n_e and c) p_e. Symbols with error bars are from Thomson scattering averaged over the 10 shot series at t=745ms and the solid line is from EMC3-EIRENE.

Figure 4: a) Electron tempeature, b) density, and c) pressure and heat flux at the outer target mapped to the midplane from Langmuir probes (circles) and EMC3-EIRENE (solid lines) averaged over toroidal angle for the 10 shot series. Red crosses are upstream data from Thomson scattering.

Figure 5: Fractional change in electron pressure at the outer target at $\rho \approx 3$mm from experiment (symbols) and EMC3-EIRENE (dashed line).

Figure 6: N^{+4} density at the toroidal angle of the puff with three N V spectroscopic views shown (dashed lines). Arrows indicate dominant forces in the regions shown.

Figure 7: Fractional change in N V line emission from experiment (symbols) and EMC3-EIRENE (dashed lines).

Figure 8: Heat flux at the outer target plate as calculated by EMC3-EIRENE.

Figures

Figure 1: (75x50mm)

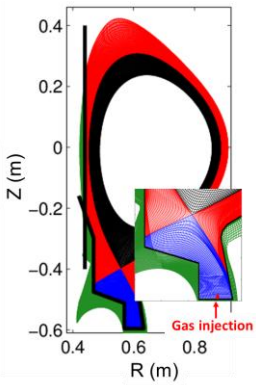

Figure 2: (75x30mm)

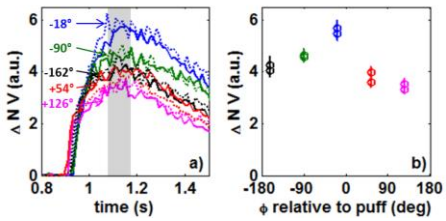

Figure 3: (75x26mm)

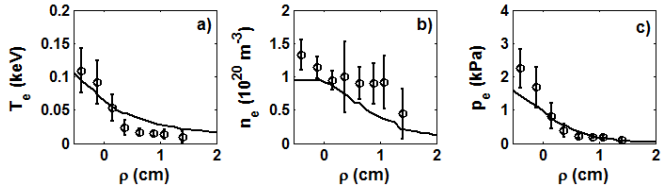

Figure 4: (75x50mm)

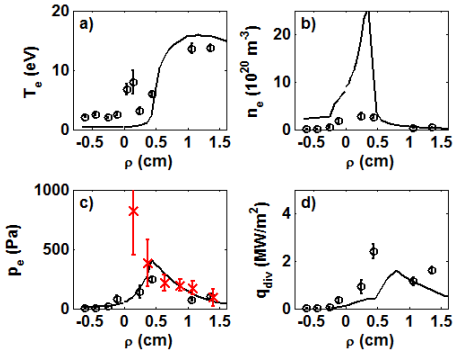

Figure 5: (75x30mm)

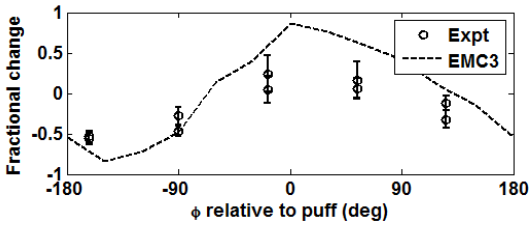

Figure 6: (75x50mm)

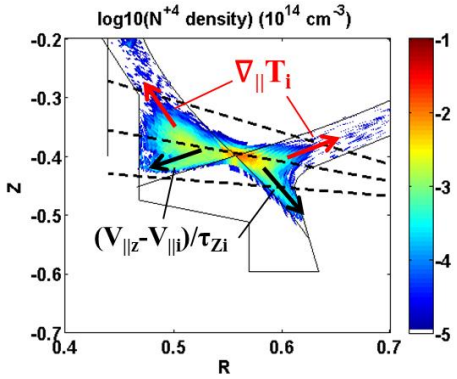

Figure 7: (75x55mm)

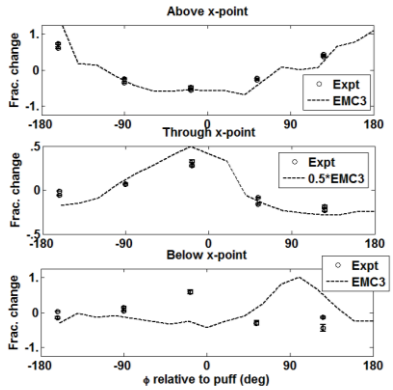

Figure 8: (75x50mm)